

# The Microscopic Structure of Liquid Methanol from Raman Spectroscopy

Ke Lin,<sup>†</sup> Xiaoguo Zhou,<sup>†</sup> Yi Luo,<sup>\*,†,‡</sup> and Shilin Liu<sup>\*,†</sup>

Hefei National Laboratory for Physical Sciences at the Microscale, Department of Chemical Physics, University of Science and Technology of China, Hefei, Anhui 230026, China; and Department of Theoretical Chemistry, School of Biotechnology, Royal Institute of Technology, S-10691 Stockholm, Sweden

Received: May 28, 2009; Revised Manuscript Received: February 5, 2010

The microscopic structure of liquid methanol has been systematically investigated with Raman spectroscopy in a temperature range of 15–55 °C. The unbonded free –OH stretching vibrational band has been observed at  $\sim 3660\text{ cm}^{-1}$  in pure liquid. With the aid of depolarization measurements and theoretical calculations, four featured spectral components have been unambiguously identified and assigned to four well-defined vibrational modes of clusters in chain or ring forms. Furthermore, the cluster size distribution and its temperature dependence have been derived from the spectral fittings for the first time, which lead to the conclusion that the trimer, tetramer, and pentamer are the dominant clusters in liquid methanol, taking up more than 50% of total clusters.

## 1. Introduction

Water and alcohols are the mostly used liquids in our daily life. Very little is known about the real structure of liquid water because of its complicated hydrogen-bonding networks. The smallest alcohol, methanol, with a simpler structure can form much fewer hydrogen bonds than water. However, its microscopic structure in the liquid phase has long been under debate due to the lack of a proper description of hydrogen-bonding network. Linus Pauling proposed in his famous book, *The Nature of the Chemical Bond* (third ed., Cornell Univ. Press: Ithaca, NY, 1960), that the dominant structure in liquid methanol should be cyclic hexamer. His view has both been supported and contested by subsequent studies, the competing interpretation being that the majority of liquid molecules are ordered in chains with up to 10 members or linear trimer–tetramer chains. Over the years, limited structural information under certain temperatures has been obtained experimentally by X-ray and neutron diffraction<sup>1–5</sup> as well as X-ray absorption/emission<sup>6–8</sup> techniques, and theoretically by molecular dynamics/Monte Carlo simulations.<sup>9–14</sup> Although it is now believed that methanol molecules form clusters in chains<sup>1,2,4,8–14</sup> or rings<sup>3,15,16</sup> in the liquid phase, there is no consensus on the size distribution of the clusters. What the dominant cluster size in liquid methanol should be has been an issue under intensive debate. For instance, different dominant structures, such as trimer and tetramer chains,<sup>1,2</sup> hexamer chain,<sup>4</sup> or hexamer ring,<sup>3</sup> have been proposed from neutron diffraction experiments. Molecular dynamics simulations have long been regarded as the ultimate solution for determination of liquid structures but unfortunately have offered a variety of choices for the averaged size, varying from 4,<sup>9</sup> 5–6,<sup>13</sup> 7–9,<sup>10</sup> 10,<sup>14</sup> 11,<sup>12</sup> to 10–12.<sup>11</sup>

Raman spectroscopy is a classic and powerful experimental tool that has been widely used to determine the microscopic structure and dynamics of liquid molecular systems. It is a nondestructive probing technique that can provide intrinsic structure information of the systems. One of the recent examples

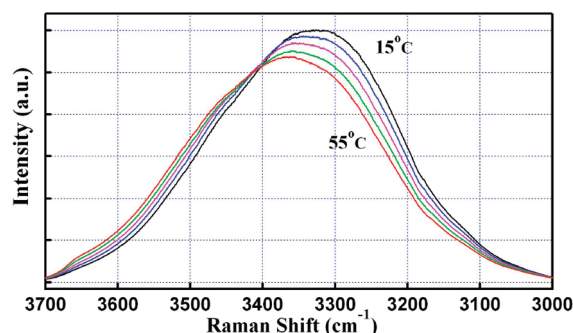


**Figure 1.** Raman spectra of liquid  $\text{CD}_3\text{OH}$  in the –OH stretching region under temperatures of 15 °C (black), 25 °C (blue), 35 °C (purple), 45 °C (green), and 55 °C (red). The weak interference from the overtone of – $\text{CD}_3$  stretching vibrations in this region has been subtracted with the spectral data of  $\text{CD}_3\text{OD}$  at each temperature. Measurements were made with the excitation laser at 532 nm (vertically polarized, unpolarized collection).

is the Raman spectral study on liquid water,<sup>17,18</sup> which has convincingly demonstrated that the conventional four-hydrogen-bonded liquid water structure should still hold and the introduction of the controversial two-hydrogen-bonded water model by X-ray absorption study<sup>19</sup> is not necessary. Here, we report a systematic study on the Raman spectra of liquid methanol under a range of temperatures, and demonstrate that rich structure information of liquid methanol can also be well provided from the study of the Raman spectra. We have unambiguously identified four featured spectral components in the –OH stretching region, and presented new assignments to them. We have found that methanol chains with averaged sizes of three to five molecules are the dominant structures (more than 50%) of liquid methanol over the temperature region 15–55 °C.

## 2. Experiments

We focused our attention on the –OH stretching vibrational modes, since they are most sensitive to the change of the hydrogen-bond (HB) network. Figure 1 shows the Raman spectrum of liquid methanol from 15 to 55 °C. To obtain pure spectra of –OH stretching vibrations, we used isotope substi-

\* Corresponding authors. E-mail: luo@kth.se (Y.L.); slliu@ustc.edu.cn (S.L.).

<sup>†</sup> University of Science and Technology of China.

<sup>‡</sup> Royal Institute of Technology.

tuted liquid methanol CD<sub>3</sub>OH, instead of normal methanol CH<sub>3</sub>OH, to eliminate the interferences from the –CH<sub>3</sub> stretching vibrations in this spectral region. We also found that when using CD<sub>3</sub>OD weak spectral features exist in the –OH stretching region, which might be from the overtone of –CD<sub>3</sub> stretching vibrations in this region. This weak interference to the Raman spectra of CD<sub>3</sub>OH was subtracted with the spectra of CD<sub>3</sub>OD at each temperature under the same experimental conditions. CD<sub>3</sub>OH and CD<sub>3</sub>OD were purchased from Cambridge Isotope Laboratories (>99.8%) and were used without further purification.

The experimental setup is similar to that used in our previous studies.<sup>20,21</sup> All of the experimental data reported in this work were obtained with a triple monochromator system (Acton Research, TriplePro) coupled to a liquid-nitrogen-cooled CCD detector (Princeton Instruments, Spec-10:100B). The precision of spectral measurement with this monochromator was estimated with the spectral lines of a mercury lamp to be better than 0.01 cm<sup>-1</sup>, and the spectral resolution was ~1.0 cm<sup>-1</sup>. The sample holder was a 10 × 10 mm quartz cell cuvette, which could be thermally controlled by a heating bath in a temperature range of 15 to 55 °C with a precision of ±0.1 °C (THD-2006, Ningbo). A cw laser (Coherent, Verdi-5W, 532 nm) was used as the light source (1.0 W power at the sample). During the experiments, the incident laser was linearly polarized by using a Glan-laser prism, and its polarization direction was controlled with a half-wave plate. The Raman scattering light was collected at 90° geometry relative to the incident laser beam with a pair of *f* = 2.5 and 10 cm quartz lenses, and imaged onto the entrance slit of the monochromator for spectral dispersion. An optical depolarizer (scrambler) was inserted in between the two lenses to remove any unwanted polarization effects from the gratings of the monochromator. Spectra were typically collected at each temperature for 60s. The Raman depolarization ratio ( $\rho$ ) was measured by varying the polarization direction of the incident laser with the half-wave plate as described in ref 20.

### 3. Results and Discussion

**3.1. Raman Spectra at Different Temperatures.** Figure 1 presents our measured Raman spectra of liquid isotope substituted methanol CD<sub>3</sub>OH under different temperatures between 15 and 55 °C at 10 °C increments. The relative intensities of the –OH stretching bands were corrected by using the sharp band of symmetrical stretching of –CD<sub>3</sub> at 2075 cm<sup>-1</sup> as an internal standard which is temperature independent, and the interference from –CD<sub>3</sub> stretching vibrations was eliminated by subtracting the spectrum of CD<sub>3</sub>OD. A noticeable temperature effect on the OH band profile was clearly observed. As seen from Figure 1, the temperature-dependent spectra intersect at the same point, ~3405 cm<sup>-1</sup>, which is the so-called “isosbestic point” (temperature invariant point).<sup>22</sup> The isosbestic point commonly exists in the temperature-dependent Raman and infrared absorption spectra of hydrogen-bond-containing systems, and its meaning has been extensively discussed for the liquid water system.<sup>23,24</sup> The existence of an isosbestic point has often been interpreted as a result of a two-state behavior of interconverting chemical or structural species upon changes of temperature.<sup>22–28</sup> Recently, an alternative microscopic origin was proposed that the isosbestic point can arise from the statistical thermal distribution of harmonic oscillators in a continuous distribution of structures, and therefore should not be used as evidence or fingerprint of multistate (discrete cluster distribution) behavior.<sup>17,18</sup>

The temperature-dependent Raman spectra of liquid methanol in the –OH stretching region have already been recorded for

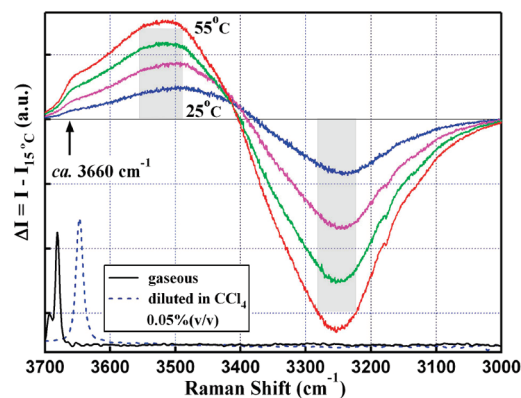


**Figure 2.** Difference Raman spectra of liquid CD<sub>3</sub>OH relative to the spectrum at 15 °C ( $\Delta I = I - I_{15^\circ\text{C}}$ ) which shows two bands with different temperature dependences as marked by shadow blocks, a temperature increasing band at 3550 cm<sup>-1</sup>, and temperature decreasing band at 3250 cm<sup>-1</sup>. A small shoulder marked with an arrow at ~3660 cm<sup>-1</sup> has been clearly observed, indicating the existence of non-H-bonded –OH (free –OH) in liquid methanol. For comparison, the Raman spectra of gaseous CD<sub>3</sub>OH (black solid line) and that diluted in CCl<sub>4</sub> solvent (0.05% v/v, blue dashed line) were also shown in the figure.

many years,<sup>28,29</sup> but the spectral analysis was based on the so-called linear-bifurcated-trifurcated HB model in a continuously hydrogen-bonded network,<sup>29</sup> which is not consistent with the widely employed cluster model.<sup>1–17,30,31</sup> In fact, different from liquid water in which a tetrahedral H-bonding network forms, liquid methanol should be in some respects simpler than water, since much fewer hydrogen bonds can be formed in it. However, the interpretation of the broad –OH band shape from pure liquid methanol is still the subject of much discussion because of its structureless feature.<sup>18,27–40</sup> As can be seen in the following sections, it is possible to identify several spectral features from the variations of Raman spectra and depolarization ratio as a function of temperature. These features can be further assigned with the help of theoretical calculations. It is found that a linearly H-bonded cluster model seems to be the most favorable choice to interpret these new experimental findings.

**3.2. Identification of Four Components in the –OH Stretching Spectra.** The variations of –OH stretching spectra with temperatures relative to the one obtained at 15 °C are plotted in Figure 2. Similar to the case of liquid water<sup>23,26</sup> and previous studies of liquid methanol,<sup>27–29</sup> the present spectra also display a positive band with temperature increasing at around 3550 cm<sup>-1</sup> and a negative band with temperature increasing at around 3250 cm<sup>-1</sup>, which have been regarded, respectively, as indications of non-H-bonded (NHB) –OH and H-bonded (HB) –OH; the breaking of H-bonds occurring at higher temperatures corresponds to the HB → NHB process.<sup>27,28</sup>

As also can be seen in Figure 2, with the increase of temperature, a weak but apparent shoulder appears at around 3660 cm<sup>-1</sup>. For pure liquid methanol, this band had never been reported in the literature<sup>27–29,31,33,38,39</sup> but, rather, a sharp band for methanol diluted in solvents such as in CCl<sub>4</sub> or in clusters and other alcohols had been observed in this region in the Raman and IR absorption spectra,<sup>28,31–33,35–39,41,42</sup> and was considered as a fingerprint of methanol monomers and/or as terminal –OH groups in methanol chain clusters. To assign this newly observed band at ~3660 cm<sup>-1</sup>, the Raman spectra of gaseous CD<sub>3</sub>OH and liquid CD<sub>3</sub>OH diluted in CCl<sub>4</sub> solvent (0.05% v/v) have been measured for comparison. The positions of CD<sub>3</sub>OH monomer in the gas phase and in CCl<sub>4</sub> solvent are found to be at 3681 cm<sup>-1</sup> with a width of 17 cm<sup>-1</sup> and at 3647 cm<sup>-1</sup> with

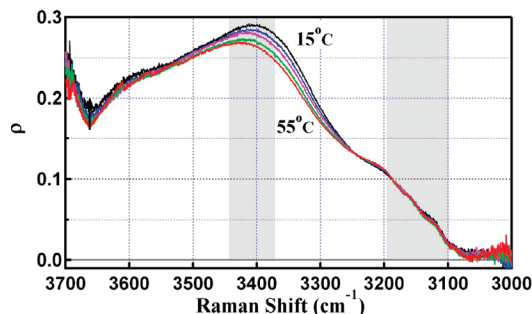


**Figure 3.** Raman depolarization ratio ( $\rho$ ) of liquid  $\text{CD}_3\text{OH}$  in the  $-\text{OH}$  stretching region under temperatures of 15 °C (black), 25 °C (blue), 35 °C (purple), 45 °C (green), and 55 °C (red). Two distinct features exist as marked by shadow blocks, a temperature-sensitive region at 3400  $\text{cm}^{-1}$ , and a region with small  $\rho$  value (close to zero) below 3200  $\text{cm}^{-1}$ . From this figure and Figure 2, a total of four featured spectral regions were identified, implying that there might be four dominant vibrational modes of clusters in liquid methanol.

a width of 48  $\text{cm}^{-1}$ , respectively. The red shift of free  $-\text{OH}$  in  $\text{CCl}_4$  relative to the gas phase (34  $\text{cm}^{-1}$ ) can be attributed to the van der Waals interactions between methanol and  $\text{CCl}_4$  molecules, which weaken the covalent  $-\text{OH}$  stretch of methanol. Considering the fact that the new band locates in between the positions of gaseous monomers and  $\text{CCl}_4$  diluted monomers, it is justified to assign it to unbonded free  $-\text{OH}$  groups of methanol monomer and/or methanol chain clusters in pure liquid. The increase of temperature breaks up more and more H-bonded clusters in liquid methanol, and raises the population of unbonded free  $-\text{OH}$  groups. As noticed from Figure 2, the frequency of free  $-\text{OH}$  stretching vibration varies with the molecular environments in the sequence  $\nu_{\text{CCl}_4}(\text{OH}) < \nu_{\text{liquid}}(\text{OH}) < \nu_{\text{gaseous}}(\text{OH})$ . In fact, it has already been pointed out that the frequency of the free  $-\text{OH}$  stretching vibrations varies with change in either alcohol or inert solvent.<sup>38,41</sup> The position of the free  $-\text{OH}$  band in  $\text{CCl}_4$  is red-shifted by 13  $\text{cm}^{-1}$  from its position in pure methanol, which implies the interactions between methanol and  $\text{CCl}_4$  molecules are stronger than those between methanol themselves. A further indication of this stronger interaction might be that the Raman signal of free  $-\text{OH}$  in 0.05% (v/v) diluted  $\text{CCl}_4$  solution is much stronger than that in the pure liquid. It can be concluded that the observed weak band at  $\sim 3660 \text{ cm}^{-1}$  provides direct evidence for the existence of unbonded free  $-\text{OH}$  in pure liquid methanol; in other words, there are methanol monomer and/or methanol chain clusters in the pure liquid methanol.

In previous studies on Raman spectra of liquid methanol, the  $-\text{OH}$  stretching band shows barely any sign of a shoulder at around 3660  $\text{cm}^{-1}$  (the expected frequency of unbonded free  $-\text{OH}$  terminal of monomers and chain clusters in liquid methanol and also the free  $-\text{OH}$  in water) even when heating up to 50 °C. This might be due to the spectral signal/noise ratio, or may be obscured by the strong  $-\text{CH}$  stretching band or by the interferences from the overtone vibrational bands in this region. The observation of free  $-\text{OH}$  groups clears up the apparent discrepancies between clusters and so-called continuum models of methanol liquid with H-bonds.<sup>27,33</sup>

In addition to the measurements of Raman spectra at different temperatures, we have also measured Raman depolarization ratios ( $\rho$ ) at different temperatures, as shown in Figure 3. Two new distinct features can be observed: one is sensitive to the change of temperature at around 3400  $\text{cm}^{-1}$ ; another has a relatively small  $\rho$  value ( $\rho \sim 0$ ) below 3200  $\text{cm}^{-1}$ . Therefore, a total of four spectral regions are identified from Figures 2

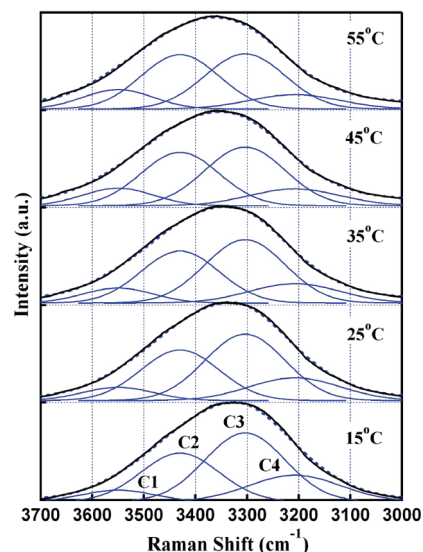


**Figure 4.** Spectral fittings to the Raman spectra of  $-\text{OH}$  stretching vibrational bands of pure liquid  $\text{CD}_3\text{OH}$  at different temperatures with four Gaussian components, C1 to C4, based on the experimentally identified four spectral components.

and 3, which present noticeable spectral or depolarization ratio differences under different temperatures. These four spectral regions should be associated with different vibrational bands. In other words, there might be four dominant vibrational modes presented in liquid methanol and the increase of temperature alters their statistical weights.

On the basis of the observation that the Raman spectrum of the  $-\text{OH}$  stretching vibrational band consists of four components, we tried to fit the spectra at different temperatures with a summation of four Gaussian profiles. It is noted that the weak unbonded free  $-\text{OH}$  band at  $\sim 3660 \text{ cm}^{-1}$  has a negligible effect on the spectral fitting. We have found that the temperature-dependent Raman spectra of liquid methanol can be well fitted with four Gaussian components, named C1–C4 and centered at 3550, 3430, 3300, and 3200  $\text{cm}^{-1}$ , respectively, as nicely shown in Figure 4. The fitted results are summarized in Table 1.

It should be mentioned that deconvolution of the broad structureless Raman spectrum of the  $-\text{OH}$  stretching band with summation of several Gaussian components would be arbitrary to some extent, if no microscopic model for the methanol liquid were preassumed. Therefore, the interpretation depends critically on the microscopic model proposed. Giguère et al.<sup>29</sup> decomposed the Raman spectra of the  $-\text{OH}$  band for liquid  $\text{CH}_3\text{OH}$  into three Gaussian components, based on a linear-bifurcated-trifurcated HB model in a continuously hydrogen-bonded network. In a recent study about the pressure effect on the hydrogen bonding in liquid  $\text{CH}_3\text{OH}$ , Arencibia et al.<sup>30</sup> used four spectral components to fit the  $-\text{OH}$  Raman spectra at a pressure of 0.1 kbar. They referred their assignments to the gaseous clusters indicated by molecular beam experiments, and assigned the four bands as monomer, dimer, trimer, and tetramer, respectively. In our study, we have experimentally identified four spectral components from the variations of Raman spectra and depolarization ratios with temperatures, and then performed spectral fittings with four components based on theoretical calculations of different methanol clusters.

**3.3. Theoretical Calculations and Interpretation of Four Spectral Components.** To identify and assign the four observed vibrational bands, we have carried out density functional theory (DFT) calculations for the Raman spectra of methanol clusters



**TABLE 1: Fitting Results to the Raman Spectra of –OH Stretching Vibrations at Different Temperatures with Four Gaussian Components Which Were Identified from the Temperature Dependences of Raman Spectra and Depolarization Ratios**

components	area					band centers/cm <sup>-1</sup>	widths/cm <sup>-1</sup>
	15 °C	25 °C	35 °C	45 °C	55 °C		
C1	605	703	796	932	1030	3550 ± 5	161 ± 8
C2	2827	2962	3043	3122	3180	3430 ± 8	178 ± 10
C3	4099	3979	3801	3520	3306	3300 ± 5	183 ± 9
C4	1800	1552	1325	1152	981	3200 ± 10	208 ± 15

with ring and chain forms. We have optimized geometric structures of gaseous methanol clusters (CD<sub>3</sub>OH)<sub>n</sub> (*n* = 2–8) in chain and ring forms using MP2 and hybrid density functional theory (B3LYP) methods with the 6-311+G(d,p) basis set as implemented in the Gaussian 03 program.<sup>43</sup> Both methods give similar results, and the optimized structures are shown in Figure 5.

It should be mentioned that the structural and energy differences between chain and ring are very small. One could imagine that, in the liquid phase, the chain and the ring could be easily interchanged. The situation is similar to liquid water, in which water molecules switch hydrogen-bonded partners through thermally activated breaking of a hydrogen bond that creates a dangling hydrogen bond before finding a new partner.<sup>44</sup> It is understandable that the observation of methanol clusters is a result of the statistical average of massive dynamic structures in liquid methanol.

On the basis of the optimized geometric structures of methanol clusters, their harmonic vibrational frequencies were calculated at the B3LYP/6-311+G(d,p) level. Comparisons between the experimentally observed and theoretically calculated vibrational frequencies of CD<sub>3</sub>OH monomer and clusters in the –OH stretching region are given in Table 2.

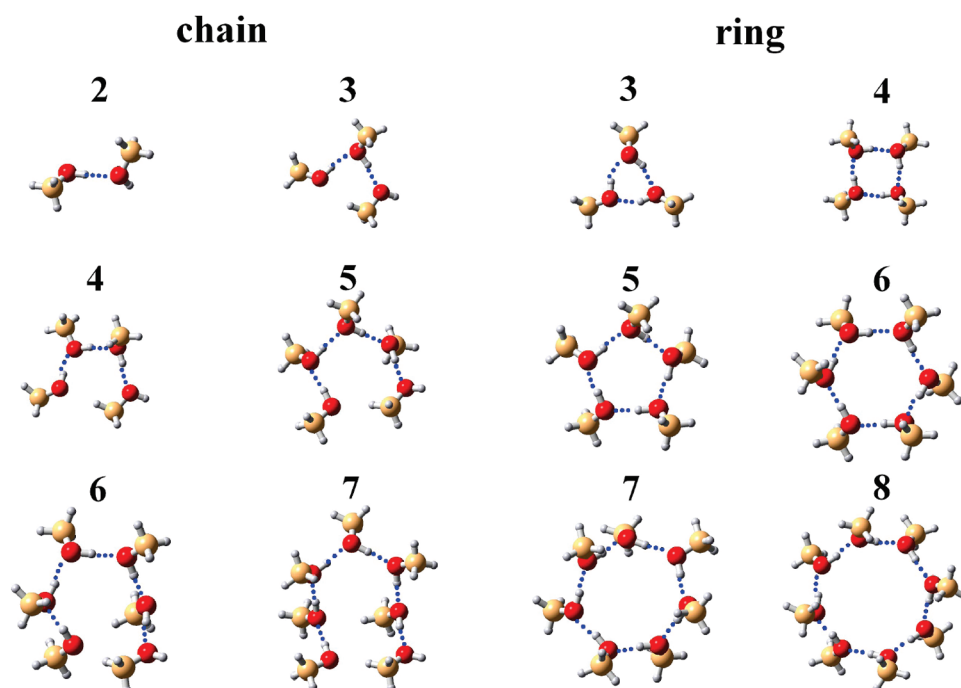
One can see that the calculated Raman frequencies agree well with the available molecular beam experimental results.<sup>45–47</sup> The Raman spectra for these methanol clusters in the liquid phase have been constructed using the calculated vibrational frequen-

**TABLE 2: Comparison between Experimentally Observed and Theoretically Calculated Vibrational Frequencies of CD<sub>3</sub>OH Monomer and Clusters in the –OH Stretching Region**

	$\nu_{\text{exp}}^a$	$\nu_{\text{calcd}}^b$	$\nu_{\text{calcd}} - \nu_{\text{exp}}$
monomer	3686	3693	7
dimer	3683	3691	8
	3574	3564	-10
ring trimer	3469	3468	-1
	3466	3459	-7
	3413	3408	-5
ring tetramer	3331	3342	11
	3294	3307	13
	3214	3223	9

<sup>a</sup> Measured vibrational frequencies in the gas phase by molecular beam experiments in ref 45. <sup>b</sup> Theoretically calculated harmonic vibrational frequencies using the Gaussian 03 software package at the B3LYP/6-311+G(d,p) level with a scaling energy factor of 0.9599.

cies and transition intensities. The apparent difference between spectra in liquid and gas phases is that, in the liquid phase, the vibrational band will shift to lower frequencies and becomes broader due to increased intermolecular interactions. Considering the observations that unbonded free –OH in liquid methanol is located at ~3660 cm<sup>-1</sup> from the difference Raman spectra in Figure 2, and that the width of free –OH for CD<sub>3</sub>OH diluted in CCl<sub>4</sub> solvent is ~50 cm<sup>-1</sup>, the calculated Raman frequencies

**Figure 5.** Optimized geometric structures of gaseous methanol clusters (CD<sub>3</sub>OH)<sub>n</sub> with *n* = 2–8 in chain and ring forms from B3LYP/6-311+G(d,p) calculations. The dotted line represents the OH···O hydrogen bond. The harmonic vibrational frequencies for these most stable clusters were obtained at the same level.

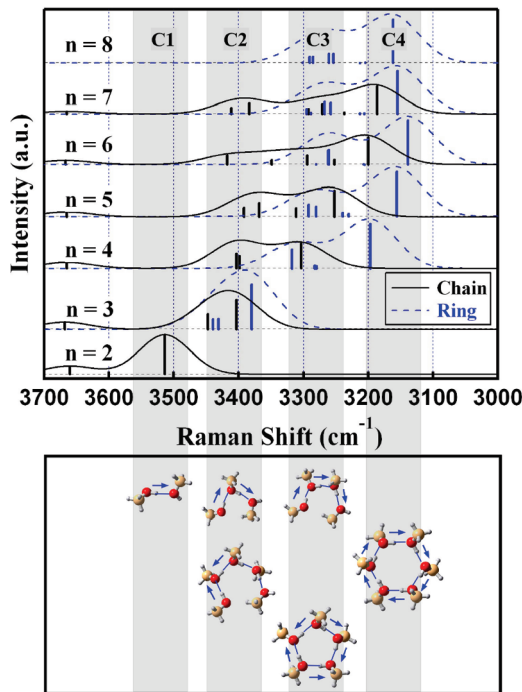


**Figure 6.** Theoretically calculated Raman spectra of  $(\text{CD}_3\text{OH})_n$  ( $n = 2-8$ ) clusters with chain (black solid) and ring (blue dashed) forms in liquid based on density functional theory at the B3LYP/6-311+G(d,p) level. The calculated spectral intensities are normalized by the number of OH groups in each cluster. To highlight the view, a Gaussian profile with a width of  $50 \text{ cm}^{-1}$  was used to convolute the spectra. The vertical bars, according to their positions, can be categorized into four groups apparently, representing different vibrational modes of  $-\text{OH}$  in clusters as schematically illustrated in the lower panel. These four groups correspond respectively to the four spectral components in Figure 4.

in the gas phase have then been uniformly lowered by  $30 \text{ cm}^{-1}$  to line up the free  $-\text{OH}$  vibrational mode at  $3660 \text{ cm}^{-1}$  in liquid methanol, and a Gaussian profile with a width of  $50 \text{ cm}^{-1}$  is employed to construct the calculated Raman spectra to mimic the real situation, as shown in Figure 6.

The calculated spectra clearly indicate that the observed small peak at  $3660 \text{ cm}^{-1}$  in Figure 2 is indeed originated from the unbonded free  $-\text{OH}$  groups in chain clusters. It is interesting to see that the calculated spectral features can also be well grouped into four regions as marked by the shadows, and their positions are consistent respectively with the four spectral components in Figure 4. This thus allows us to assign the four spectral components. The component C1 is obviously originated from the HB-related  $-\text{OH}$  stretching vibration in methanol dimer. The component C4 is related to a unique vibration associated with the in-phase stretching mode in methanol rings. Mixed in-phase and out-of-phase stretching modes in methanol chains are attributed to the component C2. For the component C3, the in-phase stretching mode of methanol chains and the out-of-phase stretching mode of methanol rings are the main contributors. These assignments are also consistent with the experimental results of depolarization ratio, e.g.,  $\rho \sim 0$  for the in-phase stretching (totally symmetric) vibration of C4 at around  $3200 \text{ cm}^{-1}$  in Figure 3. The representative vibrational modes are also schematically illustrated in the lower panel of Figure 6.

It should be mentioned that our assignments for the four spectral components in Figure 4 are different from those in the literature.<sup>29,30</sup> Since the newly observed small peak at  $3660 \text{ cm}^{-1}$  in the difference Raman spectra in Figure 2 has already been

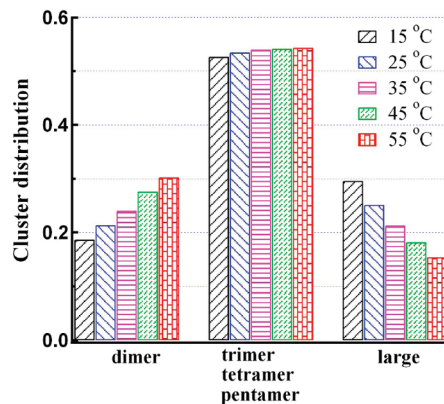


**Figure 7.** Cluster size distributions in pure liquid  $\text{CD}_3\text{OH}$  at different temperatures derived from spectral fittings and theoretical calculations.

assigned to the methanol monomer ( $3681 \text{ cm}^{-1}$  in the gas phase) and the unbonded free  $-\text{OH}$  of methanol chain clusters, the component C1 in Figure 4 should be consequently assigned to methanol dimer, rather than monomer.<sup>30</sup> In fact, the component C1 was also observed in the spectroscopic studies of  $-\text{OH}$  stretching vibrations of methanol diluted in  $\text{CCl}_4$  solvent,<sup>31,33</sup> and was assigned to the H-bonded  $-\text{OH}$  of methanol dimer from the spectral variations with methanol concentrations and temperatures. Our findings question the earlier fitting procedure used by Arencibia et al.<sup>30</sup> in their study on the pressure effect on the Raman spectra of methanol, in which the band at  $\sim 3550 \text{ cm}^{-1}$  was considered from a monomer.

**3.4. Cluster Distributions in Liquid Methanol.** The calculated spectra have provided us an opportunity to determine the cluster size distributions from the experimental spectra in Figure 4 with the help of the simple fact that the number density of a cluster is proportional to its spectral intensity. The possible vibrational modes in different regions in Figure 6 are used to fit the four spectral components in Figure 4. The fitting procedure is relatively simple by imposing two constraints. The first is that the total number of methanol molecules should be a constant for different temperatures, i.e., particle conservation law. The second one is that the final cluster distribution should be described by a normal distribution function (Gaussian distribution). A few important spectral features have also been used in the fitting. For instance, the component C1 can only be assigned to dimers. The components C2 and C3 are mostly attributed to small clusters with some contributions from long chains, while the component C4 is dominated by large ring structures.

The most stable statistical results for cluster size distribution at different temperatures are collected in Figure 7, which show that the dominant structures in liquid methanol over the measured temperature region are trimer chain/ring, tetramer chain, and pentamer chains. It can be seen that the concentration of dominant clusters is slightly dependent on temperature. The increase of temperature has resulted in the breaking down of large clusters and the increase of dimers.

These newly determined statistical distributions of cluster sizes shed new light on the microstructures of the liquid methanol. It shows that Raman spectroscopy might still be the most powerful tool to study the structures of hydrogen-bonded liquids. It is well-known that neutron diffraction experiments have had great successes in determining hydrogen-rich systems. However, for liquid methanol, the same neutron diffraction experimental results had led to a different conclusion depending on the fitting procedures used. Different dominant structures,

such as trimer and tetramer chains,<sup>2</sup> hexamer chain,<sup>4,5</sup> or hexamer ring,<sup>3</sup> were proposed. Soft X-ray absorption/emission spectra in principle should be able to provide information about the structures of hydrogen-bonded systems<sup>7,8,19</sup> However, due to the lack of detailed knowledge on the possible core-hole effects on X-ray absorption/emission processes in liquid phases, these new techniques have introduced more confusion than clarity.<sup>18,19</sup> It is believed that a comprehensive picture of liquids can only be obtained from *ab initio* or classical molecular dynamic simulations. However, due to the limited computational capacity, *ab initio* molecular dynamic simulations can still only handle relatively small samples, while classic molecular dynamic simulations are too much dependent on the force fields that are employed in the simulations. These drawbacks are particularly apparent for the structures of liquid methanol. Over the years, almost all possible results have been obtained from different dynamic simulations, which have offered a variety of choices for the averaged size, varying from 4,<sup>9</sup> 5–6,<sup>13</sup> 7–9,<sup>10</sup> 10,<sup>14</sup> 11,<sup>12</sup> to 10–12.<sup>11</sup> Chain and small ring H-bonded structures were also predicted to be the dominant structures.<sup>14,48</sup> Moreover, Monte Carlo simulations suggested that about 20% of the molecules are monomers, about one-third of the clusters contain a cyclic unit with three to four molecules, and no significant amount of hexameric rings is found.<sup>49</sup>

We are well aware that the use of DFT calculations for gas phase clusters is far from conclusive, since in our study the dynamic effects of the liquid have only been treated as a continuum average. However, this continuum model could be regarded as the first order approximation of the real situation. Most importantly, the new temperature-dependent spectral features observed in our Raman spectra of liquid methanol can be extremely useful for adjusting force fields used for molecular dynamic simulations, in particular when the direct molecular dynamic simulations for Raman spectra of liquids become reliable.

#### 4. Conclusions

In summary, we have systematically studied the temperature-dependent Raman spectra of –OH stretching vibration of liquid methanol. The unbonded free –OH stretching vibrational band has been observed at  $\sim 3660\text{ cm}^{-1}$  in pure liquid. With the help of depolarization measurements and theoretical calculations, we have unambiguously identified four featured spectral components, and presented a new assignment as four kinds of vibrational modes of clusters in chain or ring forms. Furthermore, we have derived the cluster size distribution and its temperature dependence from the spectral fittings. Trimer, tetramer, and pentamer are found to take up more than 50% of clusters in liquid. The detailed structural information obtained from this study has greatly advanced our understanding of this fundamentally important system, and may provide a good reference for theoreticians to improve their molecular dynamics models.

**Acknowledgment.** This work was supported by the National Natural Science Foundation of China (NSFC, 20873131 and 20925311), the National Key Basic Research Special Foundation (NKBRF, 2007CB815204 and 2010CB923300), and the Swedish Research Council (VR).

#### References and Notes

(1) Magini, M.; Paschina, G.; Piccaluga, G. On the structure of methylalcohol at room-temperature. *J. Chem. Phys.* **1982**, *77* (4), 2051–2056.

(2) Tanaka, Y.; Ohtomo, N.; Arakawa, K. The structure of liquid alcohols by neutron and X-ray diffraction. III. Liquid structure of methanol. *Bull. Chem. Soc. Jpn.* **1985**, *58* (1), 270–276.

(3) Sarkar, S.; Joarder, R. N. Molecular clusters and correlations in liquid methanol at room-temperature. *J. Chem. Phys.* **1993**, *99* (3), 2032–2039.

(4) Yamaguchi, T.; Hidaka, K.; Soper, A. K. The structure of liquid methanol revisited: A neutron diffraction experiment at –80 degrees C and +25 degrees C. *Mol. Phys.* **1999**, *96* (8), 1159–1168.

(5) Yamaguchi, T.; Hidaka, K.; Soper, A. K. The structure of liquid methanol revisited: a neutron diffraction experiment at –80 degrees C and +25 degrees C (vol 96, pg 1159, 1999). *Mol. Phys.* **1999**, *97* (4), 603–605.

(6) Guo, J. H.; Luo, Y.; Augustsson, A.; Kashtanov, S.; Rubensson, J. E.; Shuh, D. K.; Agren, H.; Nordgren, J. Molecular structure of alcohol-water mixtures. *Phys. Rev. Lett.* **2003**, *91* (15), 157401.

(7) Kashtanov, S.; Augustsson, A.; Rubensson, J. E.; Nordgren, J.; Agren, H.; Guo, J. H.; Luo, Y. Chemical and electronic structures of liquid methanol from x-ray emission spectroscopy and density functional theory. *Phys. Rev. B* **2005**, *71* (10), 104205.

(8) Wilson, K. R.; Cavalleri, M.; Rude, B. S.; Schaller, R. D.; Catalano, T.; Nilsson, A.; Saykally, R. J.; Pettersson, L. G. M. X-ray absorption spectroscopy of liquid methanol microjets: Bulk electronic structure and hydrogen bonding network. *J. Phys. Chem. B* **2005**, *109*, 10194–10203.

(9) Jorgensen, W. L. Quantum and statistical mechanical studies of liquids. 7. Structure and properties of liquid methanol. *J. Am. Chem. Soc.* **1980**, *102* (2), 543–549.

(10) Haughney, M.; Ferrario, M.; McDonald, I. R. Molecular-dynamics simulation of liquid methanol. *J. Phys. Chem.* **1987**, *91* (19), 4934–4940.

(11) Svishchev, I. M.; Kusalik, P. G. Structure in liquid methanol from spatial-distribution functions. *J. Chem. Phys.* **1994**, *100* (7), 5165–5171.

(12) Shilov, I. Y.; Rode, B. M.; Durov, V. A. Long range order and hydrogen bonding in liquid methanol: A Monte Carlo simulation. *Chem. Phys.* **1999**, *241* (1), 75–82.

(13) Tsuchida, E.; Kanada, Y.; Tsukada, M. Density-functional study of liquid methanol. *Chem. Phys. Lett.* **1999**, *311* (3–4), 236–240.

(14) Pagliai, M.; Cardini, G.; Righini, R.; Schettino, V. Hydrogen bond dynamics in liquid methanol. *J. Chem. Phys.* **2003**, *119* (13), 6655–6662.

(15) Ludwig, R. The structure of liquid methanol. *ChemPhysChem* **2005**, *6* (7), 1369–1375.

(16) Ludwig, R. Isotopic quantum effects in liquid methanol. *ChemPhysChem* **2005**, *6* (7), 1376–1380.

(17) Geissler, P. L. Temperature dependence of inhomogeneous broadening: On the meaning of isosbestic points. *J. Am. Chem. Soc.* **2005**, *127* (42), 14930–14935.

(18) Smith, J. D.; Cappa, C. D.; Wilson, K. R.; Cohen, R. C.; Geissler, P. L.; Saykally, R. J. Unified description of temperature-dependent hydrogen-bond rearrangements in liquid water. *Proc. Natl. Acad. Sci. U.S.A.* **2005**, *102* (40), 14171–14174.

(19) Wernet, P.; Nordlund, D.; Bergmann, U.; Cavalleri, M.; Odellius, M.; Ogasawara, H.; Naslund, L. A.; Hirsch, T. K.; Ojamae, L.; Glatzel, P.; Pettersson, L. G. M.; Nilsson, A. The structure of the first coordination shell in liquid water. *Science* **2004**, *304* (5673), 995–999.

(20) Yu, Y. Q.; Lin, K.; Zhou, X. G.; Wang, H.; Liu, S. L.; Ma, X. X. New C–H stretching vibrational spectral features in the Raman spectra of gaseous and liquid ethanol. *J. Phys. Chem. C* **2007**, *111* (25), 8971–8978.

(21) Yu, Y. Q.; Lin, K.; Zhou, X. G.; Wang, H.; Liu, S. L.; Ma, X. X. Precise measurement of the depolarization ratio from photoacoustic Raman spectroscopy. *J. Raman Spectrosc.* **2007**, *38* (9), 1206–1211.

(22) Senior, W. A.; Verrall, R. E. Spectroscopic evidence for mixture model in hot solutions. *J. Phys. Chem.* **1969**, *73* (12), 4242–4249.

(23) Walrafen, G. E.; Hokmabadi, M. S.; Yang, W. H. Raman Isosbestic points from liquid water. *J. Chem. Phys.* **1986**, *85* (12), 6964–6969.

(24) Robinson, G. W.; Cho, C. H.; Úrquidí, J. Isosbestic points in liquid water: Further strong evidence for the two-state mixture model. *J. Chem. Phys.* **1999**, *111* (2), 698–702.

(25) Walrafen, G. E.; Fisher, M. R.; Hokmabadi, M. S.; Yang, W. H. Temperature dependence of the low- and high-frequency Raman scattering from liquid water. *J. Chem. Phys.* **1986**, *85* (12), 6970–6982.

(26) Hare, D. E.; Sorensen, C. M. Raman spectroscopic study of bulk water supercooled to –33°C. *J. Chem. Phys.* **1990**, *93* (1), 25–33.

(27) Luck, W. A. P.; Fritzsche, M. The OH stretching mode and a 3 species model of liquid methanol. *Z. Phys. Chem.* **1995**, *191*, 71–86.

(28) Paolantoni, M.; Sassi, P.; Morresi, A.; Cataliotti, R. S. Raman noncoincidence effect on OH stretching profiles in liquid alcohols. *J. Raman Spectrosc.* **2006**, *37* (4), 528–537.

(29) Giguère, P. A.; Pigeon-Gosselin, M. An electrostatic model for hydrogen bonds in alcohols. *J. Solution Chem.* **1988**, *17* (11), 1007–1014.

(30) Arencibia, A.; Taravillo, M.; Perez, F. J.; Nunez, J.; Baonza, V. G. Effect of pressure on hydrogen bonding in liquid methanol. *Phys. Rev. Lett.* **2002**, *89* (19), 195504.

(31) Ohno, K.; Shimoaka, T.; Akai, N.; Katsumoto, Y. Relationship between the broad OH stretching band of methanol and hydrogen-bonding patterns in the liquid phase. *J. Phys. Chem. A* **2008**, *112* (32), 7342–7348.



- (32) Dixon, J. R.; George, W. O.; Hossain, M. F.; Lewis, R.; Price, J. M. Hydrogen-bonded forms of methanol - IR spectra and ab initio calculations. *J. Chem. Soc., Faraday Trans.* **1997**, *93* (20), 3611–3618.
- (33) Kristiansson, O. Investigation of the OH stretching vibration of CD<sub>3</sub>OH in CCl<sub>4</sub>. *J. Mol. Struct.* **1999**, *477* (1–3), 105–111.
- (34) Sokolowska, A. Influence of local molecular order on non-coincidence in the Raman spectra of methanol in liquid mixtures. I - Non-polar solvent: Carbon tetrachloride. *J. Raman Spectrosc.* **1999**, *30* (7), 507–509.
- (35) Musso, M.; Torii, H.; Ottaviani, P.; Asenbaum, A.; Giorgini, M. G. Noncoincidence effect of vibrational bands of methanol/CCl<sub>4</sub> mixtures and its relation with concentration-dependent liquid structures. *J. Phys. Chem. A* **2002**, *106* (43), 10152–10161.
- (36) Fazio, B.; Pieruccini, M.; Vasi, C. A mean field analysis of the O-H stretching Raman spectra in methanol/carbon tetrachloride mixtures. *J. Phys. Chem. B* **2005**, *109* (33), 16075–16080.
- (37) Palombo, F.; Paolantoni, M.; Sassi, P.; Morresi, A.; Cataliotti, R. S. Spectroscopic studies of the “free” OH stretching bands in liquid alcohols. *J. Mol. Liq.* **2006**, *125* (2–3), 139–146.
- (38) Max, J. J.; Chapados, C. Infrared spectroscopy of methanol-hexane liquid mixtures. I. Free OH present in minute quantities. *J. Chem. Phys.* **2008**, *128* (22), 224512.
- (39) Max, J. J.; Chapados, C. Infrared spectroscopy of methanol-hexane liquid mixtures. II. The strength of hydrogen bonding. *J. Chem. Phys.* **2009**, *130* (12), 124513.
- (40) Suhm, M. A. Hydrogen bond dynamics in alcohol clusters. In *Adv. Chem. Phys.*; John Wiley & Sons Inc: New York, 2009; Vol. 142, pp 1–57.
- (41) Kanno, H.; Honshoh, M.; Yoshimura, Y. Free hydrogen bonds in alcohol solutions with inert solvents. *J. Solution Chem.* **2000**, *29* (10), 1007–1016.
- (42) Max, J. J.; Chapados, C. Infrared spectroscopy of acetone-methanol liquid mixtures: Hydrogen bond network. *J. Chem. Phys.* **2005**, *122* (1), 014504.
- (43) Frisch, M. J.; Trucks, G. W.; Schlegel, H. B.; Scuseria, G. E.; Robb, M. A.; Cheeseman, J. R.; Montgomery, J. A., Jr.; Vreven, T.; Kudin, K. N.; Burant, J. C.; Millam, J. M.; Iyengar, S. S.; Tomasi, J.; Barone, V.; Mennucci, B.; Cossi, M.; Scalmani, G.; Rega, N.; Petersson, G. A.; Nakatsuji, H.; Hada, M.; Ehara, M.; Toyota, K.; Fukuda, R.; Hasegawa, J.; Ishida, M.; Nakajima, T.; Honda, Y.; Kitao, O.; Nakai, H.; Klene, M.; Li, X.; Knox, J. E.; Hratchian, H. P.; Cross, J. B.; Bakken, V.; Adamo, C.; Jaramillo, J.; Gomperts, R.; Stratmann, R. E.; Yazyev, O.; Austin, A. J.; Cammi, R.; Pomelli, C.; Ochterski, J. W.; Ayala, P. Y.; Morokuma, K.; Voth, G. A.; Salvador, P.; Dannenberg, J. J.; Zakrzewski, V. G.; Dapprich, S.; Daniels, A. D.; Strain, M. C.; Farkas, O.; Malick, D. K.; Rabuck, A. D.; Raghavachari, K.; Foresman, J. B.; Ortiz, J. V.; Cui, Q.; Baboul, A. G.; Clifford, S.; Cioslowski, J.; Stefanov, B. B.; Liu, G.; Liashenko, A.; Piskorz, P.; Komaromi, I.; Martin, R. L.; Fox, D. J.; Keith, T.; Al-Laham, M. A.; Peng, C. Y.; Nanayakkara, A.; Challacombe, M.; Gill, P. M. W.; Johnson, B.; Chen, W.; Wong, M. W.; Gonzalez, C.; Pople, J. A. *Gaussian 03*, revision D.01; Gaussian, Inc.: Wallingford, CT, 2004.
- (44) Eaves, J. D.; Loparo, J. J.; Fecko, C. J.; Roberts, S. T.; Tokmakoff, A.; Geissler, P. L. Hydrogen bonds in liquid water are broken only fleetingly. *Proc. Natl. Acad. Sci. U.S.A.* **2005**, *102* (37), 13019–13022.
- (45) Larsen, R. W.; Zielke, P.; Suhm, M. A. Hydrogen-bonded OH stretching modes of methanol clusters: A combined IR and Raman isotopomer study. *J. Chem. Phys.* **2007**, *126* (19), 194307.
- (46) Huisken, F.; Kulcke, A.; Laush, C.; Lisy, J. M. Dissociation of small methanol clusters after excitation of the O-H stretch vibration at 2.7 $\mu$ m. *J. Chem. Phys.* **1991**, *95* (6), 3924–3929.
- (47) Zielke, P.; Suhm, M. A. Concerted proton motion in hydrogen-bonded trimers: A spontaneous Raman scattering perspective. *Phys. Chem. Chem. Phys.* **2006**, *8* (24), 2826–2830.
- (48) Allison, S. K.; Fox, J. P.; Hargreaves, R.; Bates, S. P. Clustering and microimmiscibility in alcohol-water mixtures: Evidence from molecular-dynamics simulations. *Phys. Rev. B* **2005**, *71* (2), 024201.
- (49) Bakó, I.; Jedlovsky, P.; Palinkas, G. Molecular clusters in liquid methanol: a Reverse Monte Carlo study. *J. Mol. Liq.* **2000**, *87* (2–3), 243–254.